

Effects of homogenization and pH adjustment of cheese feed without emulsifying salt on the physical properties of high fat cheese powder

Denise Felix da Silva^{a,*}, Hao Wang^a, Tomasz Pawel Czaja^{a,b}, Frans van den Berg^a, Jacob Judas Kain Kirkensgaard^a, Richard Ipsen^a, Anni Bygvraa Hougaard^a

^a Department of Food Science, University of Copenhagen, Rolighedsvej 26, DK-1958 Frederiksberg C, Denmark

^b Department of Chemistry, University of Wrocław, 14F, Joliot-Curie, 50-383 Wrocław, Poland

ARTICLE INFO

Article history:

Received 24 June 2020

Received in revised form 2 September 2020

Accepted 2 October 2020

Available online 03 October 2020

Keywords:

High fat cheese powder

Fat structure

SAXS

LF-NMR

ABSTRACT

To enable removal of emulsifying salts (ES) in cheese powder production, the structural differences due to absence of ES on the physical and functional properties of high fat cheese powders were studied. Homogenization and pH adjustment were used to mimic ES effects. Feeds without ES showed protein aggregates and fat clusters. Non-homogenized feed without ES resulted in powder with larger particles, darker and cohesive. All parameters were improved when homogenization was applied. No significant differences were observed in powders from homogenized feeds after pH adjustment. Melting temperature and relative crystallinity were higher for the fat in powder with ES due to better fat emulsification and structure within the powder. Crystal polymorphs (α , β and β') were present in all cheese powders, β' being the dominant form. ES powder presented faster dispersion and stronger interaction with water. Thus, the absence of ES impairs the powder quality and affects the fat behavior.

© 2020 Elsevier B.V. All rights reserved.

1. Introduction

Cheese powder is an ingredient widely used in food products such as sauces, biscuits and dressings. It is produced by spray drying a uniform feed made of melted cheeses, water, and other ingredients such as emulsifying salt (ES; usually phosphates). ES is the main agent responsible for fat emulsification before spray drying. However, the trend of developing 'clean label' food ingredients led to a desire of cheese powders without emulsifying salt [1]. Cheese powders can be produced from one single type of cheese or by a combination of different cheeses, and it has been shown that the cheese type and composition, along with the addition of emulsifying salt, can strongly affect the properties of the cheese feed and consequently, the final cheese powder [1–4]. In a similar way as in cheese, the main components in cheese powder are protein and fat, but the ratio between them is highly variable depending on the cheeses used as raw material. In a cheese, the fat provides many desirable sensory properties, but also plays an important role in microstructure, texture and final application of cheese when used as an ingredient [5]. In addition, fat provides not only lubricity, texture, and mouthfeel to food products in general but also application-specific functionality, e.g. the

requirement of being in a solid state (crystallized fat) in meat, high fat bakery products, and cheese [5]. Indeed, fat crystallization is an important parameter contributing to cheese structure formation upon cooling as it is responsible for the protein - fat interactions [6]. Thus far, the main role of fat in cheese powder has not been investigated.

We have previously studied the effect of cheese maturation on cheese feed [7,8] and cheese powder properties [9,10] manufactured without emulsifying salt. However, no emphasis was given to cheese powders containing a high amount of fat (more than 50%). In high fat powders, the fat distribution and mobility during drying will also depend on how the fat is bound or structured (for instance emulsified) in the feed and subsequently, within the powder particle [11,12]. Emulsifiers are commonly used in the feed to assure that fat is bound to the protein structure in dairy based powders such as infant formula and fat-filled milk powders [12–16]. However, nowadays the inclusion of additives such as emulsifiers is no longer desired due to the requests for 'clean label' food ingredients. This makes the fat emulsification in high fat cheese powder a challenge. In the present study we thus aimed to investigate how the structural differences due to absence of emulsifying salt affected the physical and functional properties, such as powder flowability and reconstitution behavior, of high fat cheese powders. There is very limited previous research available on the role of fat in dairy powders. Therefore, emphasis was placed on understanding the structure of fat at micro-, nano- and molecular-levels.

* Corresponding author.

E-mail address: denise@food.ku.dk (D. Felix da Silva).

2. Materials and methods

2.1. Cheese powder manufacture

Cheese powders were produced by spray drying a mixture of melted cream cheese (Arla Foods Holstebro Dairy, Holstebro, Denmark) and water (the 'cheese feed') at Lactosan A/S under industrial conditions. Cheese feeds (dry matter $38 \pm 1\%$ (w/w)) were prepared by mixing and heating up to $80\text{ }^\circ\text{C}$ with direct steam for 5 min. Disodium hydrogen phosphate (BK Giulini, Ludwigshafen, Germany; denoted as ES) was used in the control formulation as 3.5% (w/w) on cheese feed basis. When applicable, the pH of the feed was adjusted using potassium hydroxide, and/or the feed was homogenized at 18 MPa. The feed was spray dried using an inlet air temperature of $190\text{ }^\circ\text{C}$ and an outlet air temperature of $60\text{ }^\circ\text{C}$. The experimental design is described in detail in section 2.6.

2.2. Cheese feed properties

2.2.1. Particle size distribution and stability

Particle size distribution was determined using a Mastersizer 3000 (Malvern Instruments Ltd., Worcestershire, UK) at $50 \pm 2\text{ }^\circ\text{C}$. The refractive index and the adsorption index for cheese feeds were set as 1.47 and 0.001 respectively. Water was used as the dispersant with a refractive index of 1.33. Drops of cheese feed were added into the dispersant chamber to a final obscuration rate between 10 and 12%. Size distribution curves showing volume intensity (%) versus size in μm were acquired. Physical stability of cheese feed was evaluated by a centrifugation method as reported previously [8].

2.2.2. Rheological properties

Rheological analyses were performed using a HAAKE RheoStress 600 rheometer (Thermo Fisher Scientific Inc., Karlsruhe, Germany) fitted with a stainless-steel bob cup geometry and rotating cone ($d = 40\text{ mm}$). During the measurements, cheese feed was kept at $50 \pm 2\text{ }^\circ\text{C}$ and approximately 30 mL of cheese feed was placed into the cup. The flow curve was measured over 15 min by an up-down shear rate sweep from 0.01 to 300 s^{-1} with a 4 mm gap. The up-curve of shear stress versus shear rate was fitted by non-linear regression using the Powder Law model (Eq. (1)) using Origin Pro 9.1 (OriginLab Corporation, Northampton-MA, USA) [10].

$$\sigma = K\dot{\gamma}^n \quad (1)$$

where K is the consistency coefficient ($\text{Pa}\cdot\text{s}^n$), and n is the flow behavior index.

2.2.3. Microstructure by CLSM

The microstructure of cheese feeds was visualized by confocal laser scanning microscopy (Leica SP5, Leica Microsystems, Wetzlar, Germany) equipped with the laser lines Krypton/Argon (488 nm) and Helium/Neon (543 nm). Fat droplets in the cheese feed were stained using Nile Red dye (9-diethylamino-5H-benzo[alpha]-phenoxazine-5-one; Sigma-Aldrich, St Louis, USA), while proteins were stained by fluorescein isothiocyanate isomer (FITC; Sigma-Aldrich, St Louis, USA). Both dyes were diluted in acetone to a final concentration of 0.01% (w/v) and 0.0045% (w/v), respectively [8]. 30 μL of each dye solution was added to a concave surface on a glass slide and dried in a fume hood. Two drops of cheese feed were added in the concave surface, mixed, cover with a glass slide and observed under $63\times$ magnification using an oil immersion objective with emission windows 500–535 nm for FITC and 580–625 nm for Nile Red [8].

2.3. Cheese powder physical properties

2.3.1. Composition, particle size distribution and color

The moisture content was determined gravimetrically via oven drying at $105 \pm 2\text{ }^\circ\text{C}$, while fat was determined by the Gerber method. Protein was quantified by Kjeldahl using a nitrogen-to-protein conversion factor of 6.38. Lactose was measured using an enzymatic method. All methods were as reported in [1] Ardö & Polychroniadou, 1999.

Particle size distribution of cheese powders was determined using a Mastersizer 3000 (Malvern Instruments Ltd., Worcestershire, UK) equipped with a dry powder disperser cell (Aero S). Around 2.0 g of powder was added in the feeding hopper, with the feeding pressure of 200 KPa. All measurements were conducted at 0.5–2% obscuration using refractive and absorption indices of 1.57 and 0.01, respectively [10]. Particle mean diameters were expressed as D [3,4] volume moment mean diameter, D [2,3] surface area mean diameter, plus D_x (10), D_x (50) and D_x (90) representing particle size in the 10%, 50% and 90% quantiles of the distribution respectively.

Color parameters L (lightness), a (redness) and b (yellowness) were measured with a Chroma Meter CR-400 (Konica Minolta Business Technologies, Inc., Tokyo, Japan) using a white calibration plate. Browning index (BI) was calculated using L , a and b as previously described [9].

2.3.2. Flowability

Flow properties of different cheese powders were evaluated using a TA.XT plus texture analyzer (Stable Micro Systems, Surrey, UK) equipped with an unconfined yield stress ring accessory and a flat probe of 50 mm diameter. A sample of 30 g of cheese powder was added into the unconfined yield stress ring. The flat plate moved downward and a selected force (1.0, 2.0 and 2.5 kg) was applied to the top of the sample, which consolidates the powder for 10 s. The unconfined yield stress ring was then removed, with the cheese powder forming a free-standing column. The flat probe subsequently moved 4 mm from the surface of the free-standing column. The flow function is given by the values for major consolidation stress (MCS) and unconfined yield strength (UYS) calculated through the Exponent software of Stable Micro Systems, which takes into consideration the cake height of the column and wall friction. The flow function coefficient (ffc) is defined as MCS divided by UYS [17].

2.3.3. Microstructure by SEM

Cheese powder microstructure was evaluated using scanning electron microscopy (SEM). A FEI Quanta 200 microscope (FEI Company, Hillsboro, USA) equipped with a back-scattered electron detector was under a voltage of 5 kV. Samples were attached by double-sided adhesive carbon tabs, mounted on the scanning electron microscopy stubs and coated with gold/palladium for 60 s before measurements.

2.4. Fat behavior in cheese powders

2.4.1. Solid fat content by LF-NMR

Solid fat content (SFC) in cheese powder samples was determined using low field magnetic resonance (LF-NMR) spectrometer (MQR Spectro-P, Oxford Instrument, Oxfordshire, UK) according to AOCS Official Method Cd 16b-93. The operating field strength was 0.47 T, resulting in a Larmor frequency of 20 MHz for ^1H . Frequency and solid fat content determination optimizations were performed using commercial standards.

2.4.2. Differential scanning calorimetry

Differential scanning calorimetry (DSC 1, Stare System, Mettler Toledo, Switzerland) was carried out to evaluate the thermal behavior of cheese powders at $21\text{ }^\circ\text{C}$. Approximately 10 mg of powder was placed in aluminum pan, held at $21\text{ }^\circ\text{C}$ for 10 min, followed by heating up to $60\text{ }^\circ\text{C}$ ($5\text{ }^\circ\text{C}\cdot\text{min}^{-1}$) (resulting in a heating curve). An empty sealed aluminum pan was used as reference during the measurements. The heat

flow ($W \cdot g^{-1}$) versus temperature of each curve was obtained and the enthalpy (ΔH) of melting was calculated by integrating the curve using Origin Pro 9.1 (OriginLab Corporation, Northampton-MA, USA).

2.4.3. X-ray scattering

Small- and Wide-angle X-ray scattering (SAXS/WAXS) profiles were measured using a GANESHA instrument from SAXSLAB (Lyngby, Denmark). The instrument uses a Rigaku (Rigaku-Denki Co., Tokyo, Japan) 40 W micro-focused Cu-source producing X-rays with a wavelength of $\lambda = 1.54 \text{ \AA}$ detected by a moveable Pilatus 300 k pixel-detector from Dectris (Baden, Switzerland) allowing different length scales to be measured. The two-dimensional scattering data were azimuthally averaged and corrected for detector in-homogeneities using standard reduction software (SAXSGUI). The radially averaged intensity I is modeled as a function of the scattering vector $q = 4\pi \sin\theta / \lambda$, where λ is the wavelength and 2θ is the scattering angle. Two instrument settings were used: a SAXS setting covering a q -range from $6 \cdot 10^{-3}$ to 0.2 \AA^{-1} and a WAXS setting covering a q -range from 0.15 to 2.75 \AA^{-1} corresponding to an upper 2θ value of 39.4 degrees or 2.27 \AA .

Relative crystallinity was calculated according to the methods described previously [18,19]. Amorphous background scattering was estimated using an iterative smoothing algorithm in MATLAB (Natick-MA, USA). The relative crystallinity was then estimated from the ratio between the area of the peak and total areas as

$$\text{relative crystallinity} = \frac{\text{area of peaks}}{\text{total area}} \quad (2)$$

where the areas are numerically integrated using in-house MATLAB functions.

2.5. Cheese powder reconstitution

2.5.1. Dispersibility

The dispersibility of cheese powder was evaluated during reconstitution at $21.0 \pm 1.0 \text{ }^\circ\text{C}$ using a Malvern Mastersizer 3000 (Malvern Instruments Ltd., Worcestershire, UK). Powders were dispersed into a 5% (5 g of powder plus 95 g of water) solution and stirred at 600 rpm. Changes in particle size upon powder reconstitution were measured after 1, 5, 15, 25, 45, 60 and 90 min. An aliquot was added to the water unit until a final obscuration of 6–8% and the particle size was measured using a refractive index of 1.57 for the powders and 1.33 for water as previously described [20,21]. The results were expressed as volume mean diameter (D_{50}) over reconstitution time.

2.5.2. LF-NMR

The reconstitution kinetics of cheese powders were monitored by ^1H low field nuclear magnetic resonance (LF-NMR) spectroscopy using MQR Spectro-P spectrometer (Oxford Instruments, Oxfordshire, UK) operating at 20 MHz for ^1H . Samples were reconstituted with distilled water (5% w/w), added into the NMR tube (18 mm o.d.) and data was recorded after 1, 5, 15, 25, 45, 60 and 90 min mixing (600 rpm). Data was collected using the Carr-Purcell-Meiboom-Gill (CPMG) sequence at $21 \pm 1 \text{ }^\circ\text{C}$. The parameters of CPMG were set as follow: recycle delay of 8 s, τ -delay of 400 μs and 1 scan. Data from 8000 echoes were acquired with a receiver gain of 5.0. Transverse relaxation times (T_{2n}) of different relaxation components were obtained using an in-house MATLAB script (Natick-MA, USA) designed for fitting the relaxation curves to a sum of exponential decays according to Eq. 3

$$I(t) = \sum_{n=1}^N M_n * e^{-t/T_{2n}} \quad (3)$$

In Eq. 3, $I(t)$ is the echo intensity as a function of time, N is the number of relaxation components, the transverse relaxation time for component n is T_{2n} , and the corresponding abundance is M_n .

Table 1
Experimental design.

Sample	Presence of emulsifying salt	pH	Homogenization
With ES	3.5% w/w ^a	5.7	no
No ES pH 6.0 non-homogenized	no	6.0	no
No ES pH 6.0	no	6.0	yes
No ES pH 5.7	no	5.7	yes

^a disodium hydrogen phosphate.

2.6. Experimental design and statistical analyses

Cheese powders were produced with different formulations as shown in Table 1. Two different approaches were included in order to mimic the effect of emulsifying salt in cheese powder manufacturing: homogenization and change in pH. Four different cheese powder formulations were investigated: (i) a control with addition of disodium hydrogen phosphate as emulsifying salt, non-homogenized (with ES), (ii) a formulation produced without emulsifying salt, pH adjusted to 6.0 and non-homogenized (No ES pH 6.0 non-homogenized), (iii) a formulation produced without emulsifying salt, pH adjusted to 6.0 and homogenized (No ES pH 6.0), and (iv) a formulation without emulsifying salt, pH adjusted to 5.7 and homogenized (No ES pH 5.7). Those conditions were chosen based on previous trials. Each powder was produced twice at an industrial scale. All analytical measurements were carried out six times. Analysis of variance (ANOVA) was performed using the Origin Pro 9.1 (OriginLab Corporation, Northampton-MA, USA) software followed by Turkey's multiple comparison test ($p \leq 0.05$).

3. Results and discussion

3.1. Cheese feed characteristics

Disodium hydrogen phosphate is an emulsifying salt commonly used in cheese powder manufacturing with the aim of obtaining a stable and homogeneous feed prior to spray drying [1,22]. It promotes, with the aid of heat and shear, physicochemical changes in the cheese protein by Ca^{2+} binding, pH adjustment and casein solubilization [6]. Previous studies have proven this effect in cheese feeds, i.e. an improved stability [22,23] followed by a reduction in size of the fat droplets and an increase in viscosity [8].

The particle size distributions (PSD) of the cheese feeds used in this investigation are shown in Fig. 1. Multimodal particle size distributions were observed for all cheese feed samples. ES feed presented three main peaks at maximum intensities around 50, 5 and 0.4 μm . As expected, the absence of homogenization in feed without emulsifying salt (No ES pH 6.0 non-homogenized) resulted in the presence of big fat droplets observed in the graph as a shoulder up to 200 μm in the PSD graphs. Feed without emulsifying salts and homogenized (No ES pH 5.7, No ES pH 6.0) exhibited two peaks with the one at 20 μm . A modest effect on the PSD was observed increasing pH from 5.7 to 6.0. This step was considered based on the hypothesis of a better casein solubilization at higher pH, and thus better fat emulsification. As expected, the particle sizes have been reduced upon homogenization.

The PSD of food emulsions are correlated with the emulsion stability. However, in this study, no phase separation was observed upon centrifugation (data not shown) as was also found in a previous study where the particle size distribution of cheese feed had no direct correlation with stability [8]. The differences in flow behavior of cheese feeds are presented in Fig. 2. The absence of emulsifying salt led to feeds with higher shear stress at a given shear rate. This behavior might be due to the presence of protein aggregates (undissolved cheese particles) as well as fat clusters, especially observed in non-homogenized samples. The consistency coefficient (K) and flow behavior index (n) values

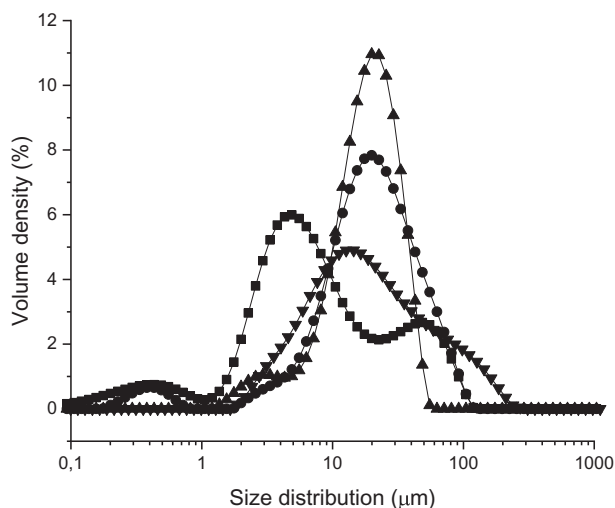


Fig. 1. Particle size distribution of cheese feeds produced with emulsifying salt (■), without emulsifying salt pH 6.0 and non-homogenized (▼), without emulsifying salt pH 6.0 homogenized (▲) and without emulsifying salt pH 5.7 homogenized (●).

estimated from the Power Law model for all samples are shown in Table 2. All feeds presented non-Newtonian shear-thinning behavior ($n < 1$), in which the apparent viscosity decreased with the increase of the applied shear rate. This behavior is related to the spatial rearrangement of protein molecules in the liquid and disruptions of their interactions. The same behavior has been observed in cheese feeds manufactured with different types of cheeses and added ingredients [1,4,8,24].

A significant increase in consistency coefficient K was observed in feeds without emulsifying salt. Within these samples, feeds with larger fat droplets presented a higher consistency coefficient and a concomitant decreased flow index, but no effect on an increase in pH was observed. Vignolles et al. 2009 investigated the viscosity and flow behavior of fat-filled milk feed and showed that an increased viscosity was related to a larger proportion of fat clusters [12]. These results contradict previous studies where a significant increase in viscosity was observed for feed containing emulsifying salt [8]. However, this difference is undoubtedly related to the large difference in gross composition, more specifically in the amount of fat and the

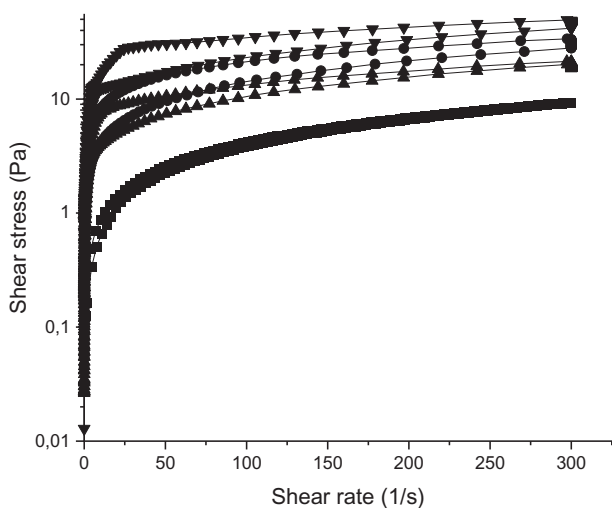


Fig. 2. Flow curves of cheese feeds produced with emulsifying salt (■), without emulsifying salt pH 6.0 and non-homogenized (▼), without emulsifying salt pH 6.0 homogenized (▲) and without emulsifying salt pH 5.7 homogenized (●).

Table 2
Power law model parameters.

Cheese feed	K (Pa·s ⁿ)	n
With ES	0.12 ± 0.03^c	0.75 ± 0.04^a
No ES pH 6.0 non-homogenized	6.77 ± 0.08^a	0.36 ± 0.00^c
No ES pH 6.0	2.32 ± 0.31^b	0.31 ± 0.02^d
No ES pH 5.7	2.73 ± 0.40^b	0.44 ± 0.01^b

With ES: cheese feed produced with emulsifying salt; No ES pH 5.7: cheese feed produced without emulsifying salt with pH adjusted to 5.7; No ES pH 6.0: cheese feed produced without emulsifying salt with pH adjusted to 6.0 and No ES pH 6.0 non-homogenized cheese feed produced without emulsifying salt with pH adjusted to 6.0 without homogenization before spray drying. K : consistency coefficient (Pa·sⁿ); n : flow index behavior. Values are means \pm standard deviation; means with different superscript letters in a column are significantly different (Tukey's HSD, $p < 0.05$).

type of cheese used as raw materials. The emulsification capacity of cheese proteins in cream cheese, as was used in the present study, might be greater due to the larger amount of intact protein present compared to matured cheeses and possibly also due to the mineral or calcium balance.

Confocal laser scanning micrographs (Fig. 3) clearly show the effect on the microstructure of the cheese feeds. As expected, feed containing ES showed a continuous and homogeneous protein structure where the fat droplets are trapped within the protein network and the presence of different sizes of fat droplets as seen in the particle size distribution is evident (Fig. 1). However, in the absence of emulsifying salts, cheese feeds showed presence of protein aggregates, void areas (black areas) and fat clusters. As previously discussed, the applied homogenization significantly decreased the size of the fat droplets within the cheese feeds. No visual difference was noticed with increasing the pH from 5.7 to 6.0. Similar results were observed in a previous study with cheese feeds containing less amount of fat [8].

3.2. Cheese powder physical properties

The composition of the cheese powders is shown in Table 3. The bulk composition of a dairy powder is directly correlated with feed composition [25,26]. As expected, all cream cheese powders showed a high amount of fat, and significant amounts of lactose when compared to alternative types of cheeses powders [3,21,24]. Moreover, the powder physical characteristics such as particle size, color, flowability and microstructure can also be affected by feed viscosity, spray drying procedure, powder composition and the interaction between components. In this study, the size of powder particles and color parameters were measured as well and are given in Table 3.

The absence of emulsifying salt and homogenization led to increased particle sizes in powder No ES pH 6.0 non-homogenized; this might be due to the higher viscosity of the feed and inhomogeneity of samples. It has been shown that impaired atomization caused by high viscosity may lead to larger particles in spray dried food ingredients. This effect has been seen before in both milk protein concentrates and infant formula feeds [15,27]. To some extent a correlation between particle size in feed and particle sizes in the powder particles can be seen. Thus, larger fat droplets in the feed, together with higher viscosity, led to bigger particles in the powder.

Both powders No ES pH 6.0 and No ES pH 5.7 showed smaller D [3,4] and more homogeneous size distribution observed by the narrow range between the percentiles $D_x(10)$ and $D_x(90)$. A significantly ($p < 0.05$) higher D [3,4] was seen in ES powder. The size of particles might also affect their color, which is an important quality characteristic for cheese powders. As a consequence of bigger particles, the color No ES pH 6 non-homogenized powder was found to be darker (lower L values), more yellow (higher b values) and consequently presented a higher browning index (Table 3). Larger particles tend to diffuse less light and consequently present lower lightness (L) [2].

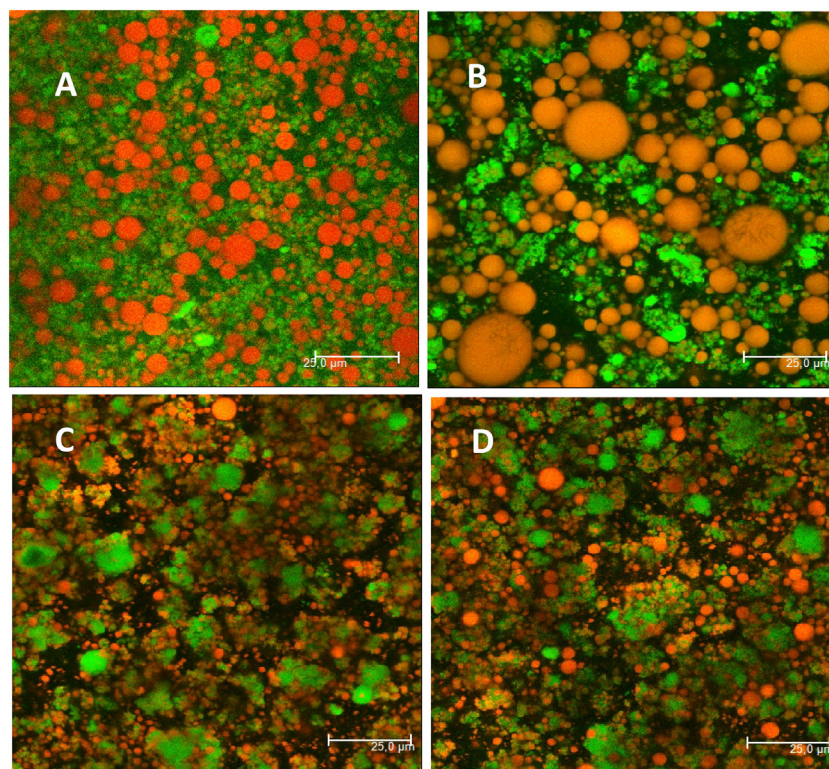


Fig. 3. Confocal laser scanning micrographs of cheese feeds. A: cheese powder produced with emulsifying salt (With ES), B: cheese powder produced without emulsifying salt with pH adjusted to 6.0 non homogenized (No ES pH 6.0 non-homogenized), C: cheese powder produced without emulsifying salt with pH adjusted to 6.0 homogenized (No ES pH 6.0) and D: cheese powder produced without emulsifying salt with pH adjusted to 5.7 homogenized (No ES pH 5.7) before spray drying. Green color represents protein and red color represents fat. (For interpretation of the references to color in this figure legend, the reader is referred to the web version of this article.)

As shown in Fig. 4, the flowability of cheese powder was characterized by its unconfined yield strength (UYS) in dependence of major consolidation stress (MCS); the ratio between MCS to UYS (the flow function coefficient) is used to characterize flowability numerically [28–30]. A good flowability in a powder is ensured when the particles can overcome the resistance to flow, flowing easily without forming lumps, clusters or aggregates. This flowability will depend on parameters such as PSD, shape, composition, temperature and powder structure [28].

In this study, ES powder presented higher flowability and was within the ‘easy flowing’ range (i.e. $4 < ffc < 10$). Yet, powders No ES pH 5.7 and No ES pH 6.0 also presented a good powder flowability in the same range, with no significant difference for different pH values. The non-homogenized powder was however classified to be within

the cohesive range ($2 < ffc < 4$). It is believed that small particle size – therefore, larger surface area – may facilitate stronger interactions between particles, reducing powder flowability. However, in this study the bigger particles sizes did not improve flowability. This might be due to the high amount of fat and larger pools of fat that can encourage the formation of bridges between particles and consequently enhance cohesion [31]. Instead, a reduction of fat content has been proven to be efficient in improving flowability in the case of milk powders [32].

3.3. Behavior of fat within high fat cheese powder

Thermal DSC profiles of cheese powder are shown in Fig. 5. Two endothermic peaks corresponding to the melting of fat were observed in all powders, suggesting the presence of crystallized fat. Broad peaks

Table 3

Gross composition, particle sizes and color parameters of cheese powders.

Cheese powder	Composition (%)				Particle size mean diameters (µm)					Color parameters			
	Moisture	Fat	Protein	Lactose	D [3,4]	D [2,3]	Dx(10)	Dx(50)	Dx(90)	L	a	b	BI
With ES	2.7	68.0	18.1	4.6	124.5 ± 1.0 ^b	84.4 ± 2.6 ^{bc}	47.3 ± 1.7 ^c	115.2 ± 2.0 ^b	214.5 ± 0.6 ^b	92.4 ± 0.1 ^a	0.9 ± 0.1 ^b	16.1 ± 0.1 ^b	19.4 ± 0.1 ^b
No ES pH 6.0 non-homogenized	2.5	63.0	23.3	5.8	254.6 ± 23.3 ^a	136.3 ± 0.57 ^a	82.3 ± 1.79 ^a	151.6 ± 3.51 ^a	303.3 ± 20.5 ^a	86.7 ± 0.5 ^d	1.2 ± 0.1 ^a	21.6 ± 0.3 ^a	29.0 ± 0.7 ^a
No ES pH 6.0	2.1	63.2	23.5	5.9	109.6 ± 2.0 ^c	87.1 ± 1.9 ^b	54.6 ± 1.3 ^b	101.6 ± 2.0 ^c	177.6 ± 2.8 ^c	89.0 ± 0.1 ^c	0.1 ± 0.1 ^d	15.5 ± 0.1 ^c	18.5 ± 0.2 ^c
No ES pH 5.7	2.4	63.4	23.7	5.9	106.0 ± 1.0 ^c	84.1 ± 0.5 ^c	52.4 ± 0.4 ^b	97.9 ± 0.8 ^c	173.3 ± 2.0 ^d	90.3 ± 0.1 ^b	0.2 ± 0.0 ^c	16.1 ± 2.0 ^b	19.2 ± 2.7 ^b

With ES: cheese powder produced with emulsifying salt; No ES pH 5.7: cheese powder produced without emulsifying salt with pH adjusted to 5.7; No ES pH 6.0: cheese powder produced without emulsifying salt with pH adjusted to 6.0 and No ES pH 6.0 non homogenized: cheese powder produced without emulsifying salt with pH adjusted to 6.0 without homogenization before spray drying. D [3,4] volume moment mean diameter, D [2,3]: surface area mean diameter, Dx(10), Dx(50) and Dx(90) represent particle size in the 10%, 50% and 90% quantiles of the distribution respectively. L: lightness, a: redness, b: yellowness and BI: browning index. Values are means ± standard deviation; means with different superscript letters in a column are significantly different (Tukey's HSD, $p < 0.05$).

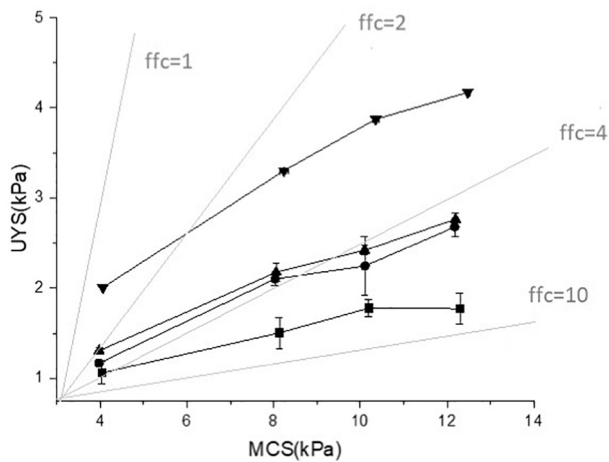


Fig. 4. Flow functions of cheese powders produced with emulsifying salt (■), without emulsifying salt pH 6.0 and non-homogenized (▼), without emulsifying salt pH 6.0 homogenized (▲) and without emulsifying salt pH 5.7 homogenized (●) derived from unconfined yield strength (UYS) and major consolidation stress (MCS). ffc: flow function coefficient.

imply that the fat crystals are heterogeneous, indicating that the melting of the different crystals occurs over a range of temperatures. Also, the presence of multiple peaks indicates the melting of different

polymorphic forms [5]. The first endothermic peak was found at 24.8 °C for all powders. Contrary, the mid-point of the second endothermic peak was found at lower temperature for powders without emulsifying salt. ES powder presented a mid-point at 39.0 °C, whereas No ES pH 6.0 non-homogenized at 37.5 °C, No ES pH 6.0 and No ES pH 5.7 showed a mid-point at 35.9 °C. These changes in the thermal profiles of the powders might be due to effect of the protein matrix and fat distribution within the powder, e.g. more surface fat (a 'wrinkled surface') can be seen in the SEM micrographs (Fig. 6) in powders without emulsifying salt. Tiensa, Barbut, & Marangoni (2017) indicated an effect of the food matrix on fat crystallization and structure in pâtés [33]. They showed a decrease in melting point of extracted fat in comparison with the fat entrapped inside the pâté matrix [33]. Similar results were found before, when milk fat in bulk presented different thermal behavior (i.e. lower melting temperature) than milk fat embedded into a protein matrix for processed cheese and cream [34].

Milk fat in cheese has three different melting fractions, corresponding to low-, mid-, and high-melting fractions. The melting profiles of processed cheeses, however, have been shown to exhibit only two melting peaks, suggesting the merging together of two of these fractions when entrapped in the protein matrix [34]. This again suggests that the food matrix and structure will exert influence on the melting behavior of fat. It is also important to note that the amount of different melting fractions in milk fat might additionally affect the melting. In the present study, samples were produced from the same batch of commercial

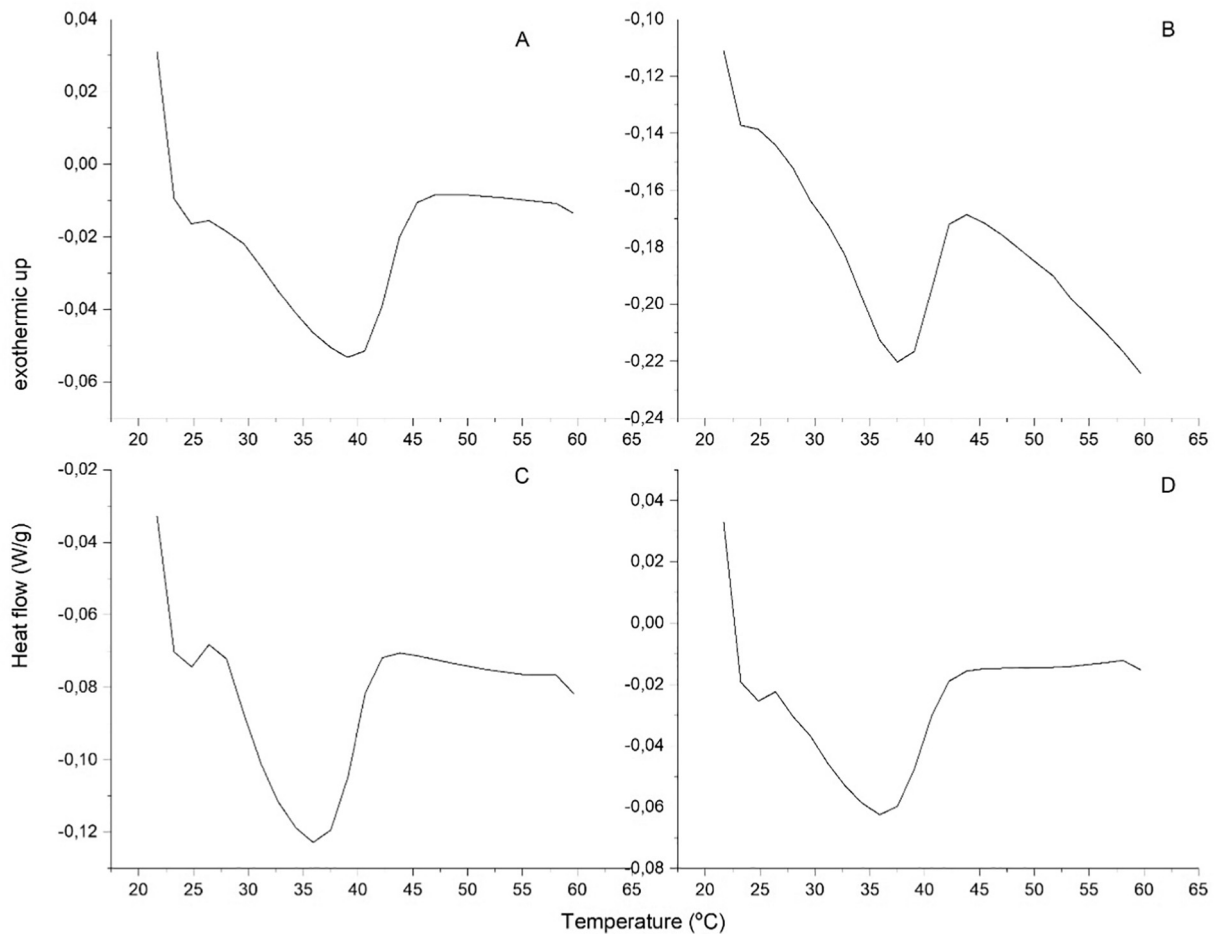


Fig. 5. Differential scanning calorimetry profiles of cheese powders. A: cheese powder produced with emulsifying salt, B: cheese powder produced without emulsifying salt with pH adjusted to 6.0 non-homogenized, C: cheese powder produced without emulsifying salt with pH adjusted to 6.0 homogenized, and D: cheese powder produced without emulsifying salt with pH adjusted to 5.7 homogenized before spray drying.

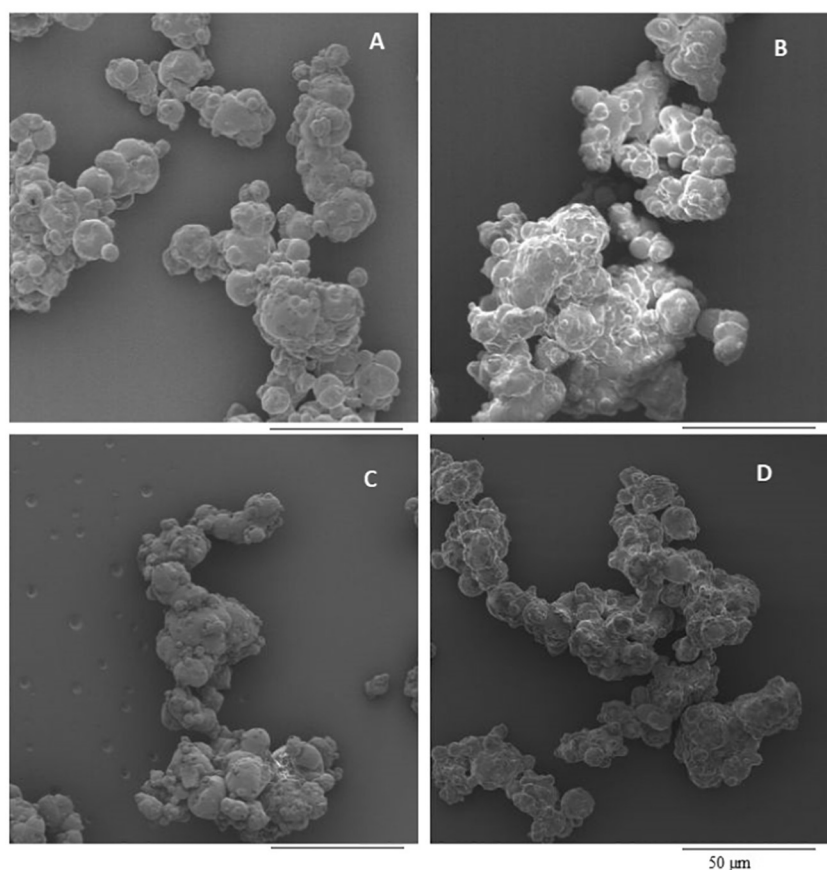


Fig. 6. Scanning electron micrographs of cheese powders. A: cheese powder produced with emulsifying salt (With ES), B: cheese powder produced without emulsifying salt with pH adjusted to 6.0 non homogenized (No ES pH 6.0 non-homogenized), C: cheese powder produced without emulsifying salt with pH adjusted to 6.0 homogenized (No ES pH 6.0) and D: cheese powder produced without emulsifying salt with pH adjusted to 5.7 homogenized (No ES pH 5.7) before spray drying.

cream cheese used as raw material. We therefore do not expect significant differences in this regard, and the homogeneous distribution of fat within feed and powder could be responsible for the higher observed melting point in the with ES powder (Fig. 5).

The percentage of solid fat content (SFC) is presented in Table 4. More solid fat was found in ES powder ($33.1 \pm 0.1\%$), followed by No ES pH 6.0 non-homogenized at $32.9 \pm 0.5\%$. Likewise, the enthalpy per gram of fat (Table 4) has been shown previously to be correlated to the amount of solid fat, suggesting that less fat crystals were present to be melted, and thus less energy was required [47].

The structure of fat in cheese powder was investigated at nano- and molecular-scale using small- and wide-angle X-ray scattering. The full scattering curve (Fig. 7) showed that there were three structural regimes in all powders. Wide-angle x-ray scattering (WAXS) spectra can

Table 4
Enthalpy of melting (J/g fat) and percentage of solid fat content (SFC) in cheese powders.

Cheese powder	Enthalpy (J/g fat)	SFC (%)
With ES	23.9 ± 1.3^c	33.1 ± 0.1^a
No ES pH 6.0 non homogenized	20.0 ± 0.2^b	32.9 ± 0.5^a
No ES pH 6.0	20.7 ± 1.5^{ab}	31.0 ± 0.2^b
No ES pH 5.7	20.7 ± 2.4^{ab}	27.2 ± 0.2^c

With ES: cheese powder produced with emulsifying salt; No ES pH 5.7: cheese powder produced without emulsifying salt with pH adjusted to 5.7; No ES pH 6.0: cheese powder produced without emulsifying salt with pH adjusted to 6.0 and No ES pH 6.0 non homogenized: cheese powder produced without emulsifying salt with pH adjusted to 6.0 without homogenization before spray drying.

Values are means \pm standard deviation; means with different superscript letters in a column are significantly different (Tukey's HSD, $p < 0.05$).

be used to identify the presence of different polymorphic forms, whereas the small-angle x-ray scattering (SAXS) scattering region allows for determination of the size or thickness of the triacylglycerol lamellae [5]. One of the regimes can be assigned to the lamellar packing of the fat in the system which gives rise to peaks around $q \sim 0.1$ to 0.6 \AA^{-1} . The main first order lamellar peak at $q = 0.151 \text{ \AA}^{-1}$ shows that the fat is packed in a 2 L configuration with a repeat distance of 41.6 \AA and this applies to all four powders suggesting very similar triacylglycerol composition. The same conformation has been identified in processed cheeses [34,35] and in Emmental cheeses [36].

At higher q -values in Fig. 7 the chain-chain structure can be observed and the scattering was dominated by a broad amorphous peak with a number of crystal peaks on top. Three crystal polymorphic forms were identified in the cheese powders with a d -spacing of 4.15 \AA for α , 4.6 , 3.85 and 3.7 \AA for β , and 4.2 and 3.8 \AA for β' crystals. The main fat polymorph was the β' configuration although there might be traces of α and β polymorphs in all samples. The origin of the peak at $q = 0.825 \text{ \AA}^{-1}$ is currently unknown, but it is not a higher order lamellar peak. Although all samples show β' crystals, there is a small difference in the positions of the β' peaks indicating that the chain packing is slightly more compressed in the homogenized samples without ES. The relative crystallinity was highest in the with ES sample (1.74%) and roughly equal in the rest: 1.45% for No ES pH 6.0 non-homogenized, 1.50% for No ES pH 6.0 and 1.47% for No ES pH 5.7. These results also correlate with the melting temperature and enthalpy as shown in Table 4.

Studies have shown the presence of β crystals when milk fat was entrapped into a protein matrix, which is rarely the case in bulk milk fat [5,34,37]. These studies suggested that the physical constraints

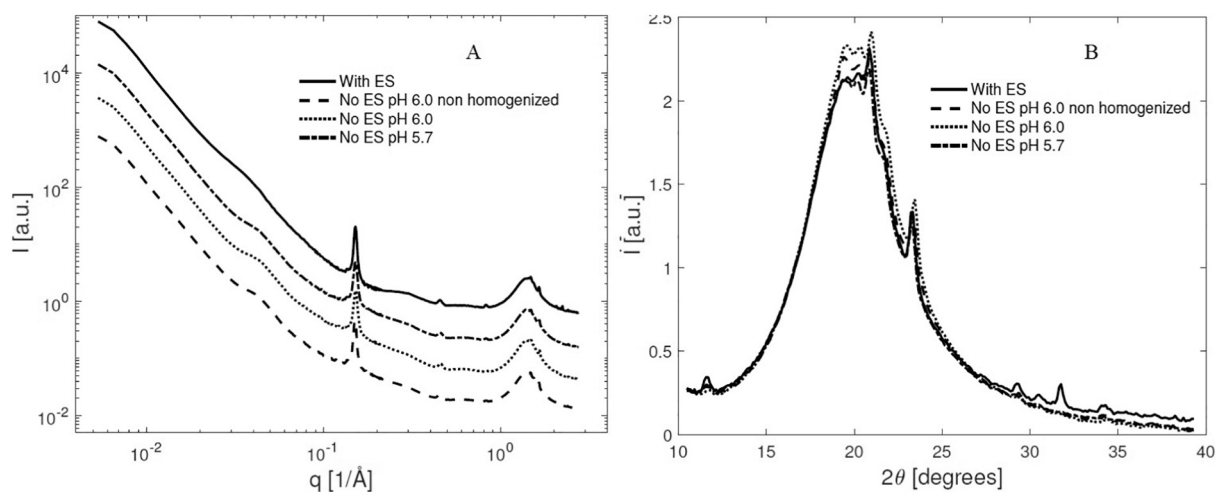


Fig. 7. Full scattering curve of SAXS/WAXS data (A) and zoom of WAXS data (B) for the cheese powder produced with emulsifying salt; cheese powder produced without emulsifying salt with pH adjusted to 5.7, cheese powder produced without emulsifying salt with pH adjusted to 6.0; cheese powder produced without emulsifying salt with pH adjusted to 6.0 without homogenization before spray drying.

imposed by the solid food matrix could have forced the triacylglycerol in milk fat to arrange into the most compact or stable form [34,38,39].

The third structural regime is the large-scale nanostructure, which is probed for $q < 0.1 \text{ \AA}^{-1}$. It was found that all samples had a clear feature around $q \sim 0.04 \text{ \AA}^{-1}$ indicating a characteristic length scale of around 14–20 nm, where for processed cheeses a domain size of 19–23 nm has been identified previously [34]. This suggests a more compacted packing in cheese powder, compared to processed cheeses, and therefore, a more stable polymorphism. However, in the three samples without emulsifying salt this packing was very similar, while the ES powder has a feature shifted to a lower q which was less pronounced. This indicates that the emulsifying salt caused a loosening of the nano-structural arrangement responsible for this feature.

3.4. Reconstitution behavior

Bearing in mind that cheese powders are dissolved before use as an ingredient in food formulations, their ability to rehydrate or reconstitute readily in water is essential. It is well known that reconstitution of powder is a dynamic process [40] that can be divided in several stages such as wettability, swelling, sinkability, dispersibility and dissolution [41,42]. Changes in the particle size distribution during reconstitution of cheese powders in water are shown in Fig. 8. This method has been used to understand the dispersibility of many dairy powders, including cheese powders, where the size of the dispersing particles decreases upon reconstitution in water. The dispersibility can thus be quantified by the rate of decrease in particle size $D_x(50)$ [9,21,43,44]. Comparing the reconstitution kinetics profiles of the four samples it was observed that the addition of emulsifying salt had a significant effect on the dispersibility of powder. After 1 min of reconstitution, ES powder showed particles around $9.0 \pm 0.9 \mu\text{m}$, whereas powders without emulsifying salt exhibited significantly bigger particles i.e. $96.9 \pm 4.0 \mu\text{m}$ for No ES pH 6.0 non-homogenized, with a decrease for No ES pH 6.0 to $93.07 \pm 3.7 \mu\text{m}$ and a decrease for No ES pH 5.7 to $85.9 \pm 1.3 \mu\text{m}$. A faster decay was seen for No ES pH 6.0 non-homogenized, but after 90 min reconstitution no differences was observed in particle size of powder without emulsifying salts with sizes of 10.7 ± 0.3 , 8.4 ± 2.1 , $10.1 \pm 6.0 \mu\text{m}$ for No ES pH 6.0 non-homogenized, No ES pH 6.0 and for No ES pH 5.7, respectively. ES powder ended up at $5.5 \pm 0.4 \mu\text{m}$ after 90 min, indicating a significantly better dispersibility of powders upon addition of emulsifying salt.

Low field nuclear magnetic resonance (LF-NMR) was also used to assess the reconstitution kinetics based on the strength of water binding

in cheese powders upon reconstitution. Transverse relaxation times (T_{21} and T_{22}) and the corresponding relative abundance populations (M_1 and M_2) after bi-exponential fitting of the CPMG curves are shown in Fig. 9. Two proton populations were observed during reconstitution for all powders, indicating the presence of two water fractions with distinct different mobility. T_{21} represents the less mobile fraction with values between 100.0 and 106.0 ms, which can be assigned to the water fraction bound to protein [3,45], whereas T_{22} represents the more mobile fraction. Upon reconstitution, the relaxation time for both fractions decrease, indicating greater interaction between the water and the cheese powders, i.e. a rehydration process.

After 1 min of reconstitution in water, ES powder showed the lowest values for T_{21} indicating a stronger interaction compared to the powders without emulsifying salt that showed significantly higher T_{21} values (Fig. 9). This behavior might be related to the better solubilization of caseins due to the action of emulsifying salts on the proteins, therefore being easier to rehydrate. After 90 min, no significant difference was found. These results complement the data from the

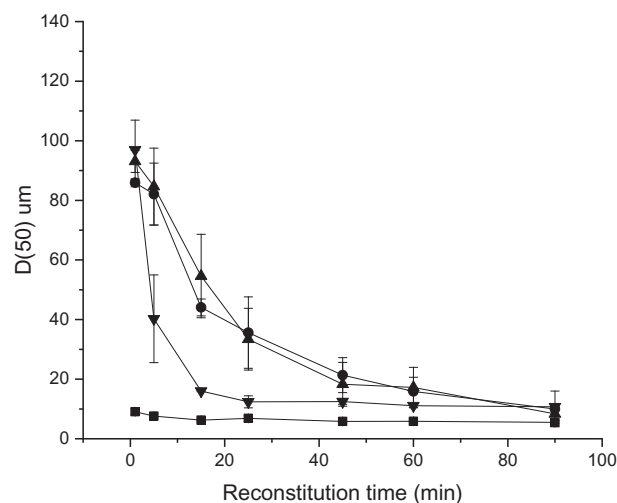


Fig. 8. Dispersibility of cheese powders upon reconstitution at $20.0 \pm 1.0 \text{ }^\circ\text{C}$. Cheese powders produced with emulsifying salts (■), without emulsifying salts and non-homogenized (▼), without emulsifying salts pH 6.0 homogenized (▲) without emulsifying salt pH 5.7 and homogenized (●).

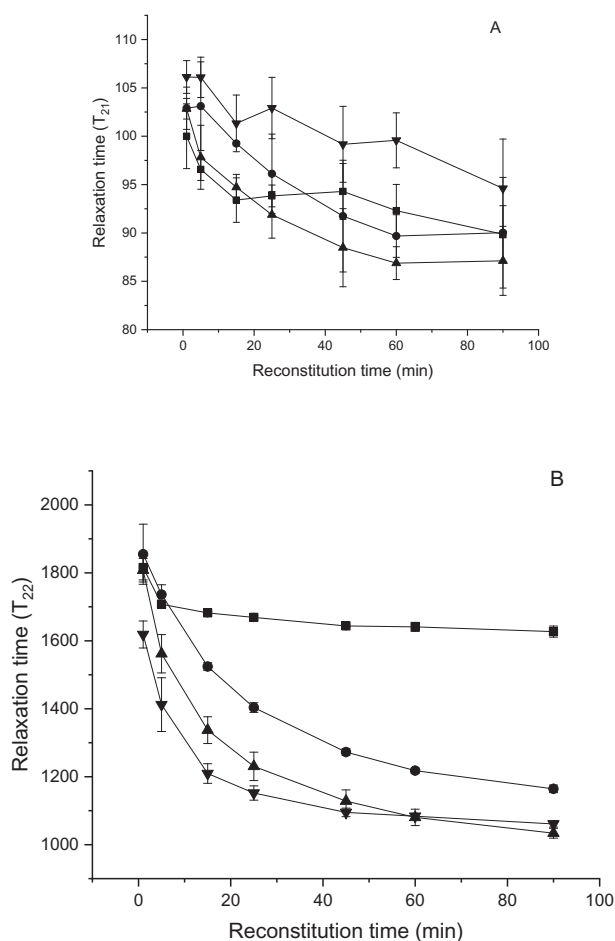


Fig. 9. Reconstitution kinetics of cheese powders for less mobile T_{21} (A) and more mobile T_{22} (B) proton populations based on CPMG measurements.

dispersibility measurements, where the ES powder showed smaller particles in the beginning of reconstitution (Fig. 8).

The second water fraction relaxation time (T_{22}) decreased significantly in powders without emulsifying salt over reconstitution time, indicating the rehydration was continuing for a longer time in those powders, whereas ES has reached a constant value after 15 min (Fig. 9). Likewise, the relative abundance of the more mobile component (M_{22}) increased over time (data not shown). The reconstitution behavior of high fat cheese powders has not been studied before. However, previous studies suggested a significant effect on the ingredients addition, cheese age and presence of lactose in the reconstitution of cheese powders [9,25].

4. Conclusions

Absence of emulsifying salt in high fat cheese powder significantly affected the rheological and microstructural properties of cheese feeds. When applying homogenization and pH adjustment in cheese feed produced without emulsifying salt to mimic the emulsifier function, these feeds exhibited protein aggregation and fat clusters. Homogenization significantly decreased the fat clusters and the consistency coefficient but no effect was observed in the microstructure or rheological behavior of homogenized feed upon changes in pH. Cheese powder properties such as particle size distribution, color, flowability, plus thermal and reconstitution behavior were also affected. Feed without emulsifying salt and non-homogenized resulted in a powder with larger particles, darker (lower L) and more yellow (higher b) in appearance

and higher cohesiveness observed by a reduced flowability. A substantial improvement was obtained when the feed was homogenized, no significant differences were observed between powders after pH was adjusted from 5.7 to 6.0. The melting behavior of the fat in cheese powder depends on the powder structure, and powder containing emulsifying salt showed a higher melting temperature as well as increased solid fat content and relative crystallinity. This might be due to the better fat emulsification or fat crystal network structure within the powder. The fat in all powders was shown to be packed in a 2 L configuration suggesting very similar triacylglycerol composition. The β' crystal form was the most predominant, although traces of α and β were present in all samples. Powders produced with emulsifying salt presented faster dispersion as well as stronger interaction with water observed by the decrease in relaxation time of both water fractions measured using the LF-NMR method; after 90 min of reconstitution no differences were observed between any of the samples.

Declaration of Competing Interest

The authors declare no conflict of interest.

References

- [1] D. Felix da Silva, C. Hirschberg, L. Ahrné, A.B. Hougaard, R. Ipsen, Cheese feed to powder: effects of cheese age, added dairy ingredients and spray drying temperature on properties of cheese powders, *J. Food Eng.* 237 (2018) 215–225, <https://doi.org/10.1016/j.jfoodeng.2018.05.015>.
- [2] N. Koca, Z. Erbay, F. Kaymak-Ertekin, Effects of spray-drying conditions on the chemical, physical, and sensory properties of cheese powder, *J. Dairy Sci.* 98 (2015) 2934–2943, <https://doi.org/10.3168/jds.2014-9111>.
- [3] D. Felix da Silva, F.H. Larsen, A.B. Hougaard, R. Ipsen, The influence of raw material, added emulsifying salt and spray drying on cheese powder structure and hydration properties, *Int. Dairy J.* 74 (2017) 27–38, <https://doi.org/10.1016/j.idairyj.2017.01.005>.
- [4] M. Uргу, S. Unluturk, N. Koca, Effects of fat reduction on the stability, microstructure, rheological and color characteristics of white-brined cheese emulsion with different emulsifying salt amounts, *Korean J. Food Sci. Anim. Resour.* 38 (2018) 866–877, <https://doi.org/10.5851/kosfa.2018.e8>.
- [5] K.D. Mattice, A.G. Marangoni, Fat crystallization and structure in bakery, meat, and cheese systems, in: *Struct. Anal. Edible Fats*, AOCS press, 2018: pp. 287–311. doi: <https://doi.org/10.1016/B978-0-12-814041-3.00010-1>.
- [6] P.F. Fox, T.P. Guinee, T.M. Cogan, P.L.H. McSweeney, *Fundamentals of Cheese Science*, 1st ed. Aspen Publishers, Inc, Gaithersburg, 2000.
- [7] C. Ray, A. Gholamhosseinpour, R. Ipsen, A. Hougaard, The effect of age on Cheddar cheese melting, rheology and structure, and on the stability of feed for cheese powder manufacture, *Int. Dairy J.* 55 (2016) 38–43, <https://doi.org/10.1016/j.idairyj.2015.11.009>.
- [8] A. Kelimu, D. Felix da Silva, X. Geng, R. Ipsen, A.B. Hougaard, Effects of different dairy ingredients on the rheological behaviour and stability of hot cheese emulsions, *Int. Dairy J.* 71 (2017) 35–42, <https://doi.org/10.1016/j.idairyj.2017.02.005>.
- [9] D. Felix da Silva, D. Tziouri, L. Ahrné, N. Bovet, F.H. Larsen, R. Ipsen, A.B. Hougaard, Reconstitution behavior of cheese powders: effects of cheese age and dairy ingredients on wettability, dispersibility and total rehydration, *J. Food Eng.* 270 (2020) <https://doi.org/10.1016/j.jfoodeng.2019.109763>.
- [10] D. Felix da Silva, C. Hirschberg, L. Ahrné, A. Hougaard, R. Ipsen, Cheese feed to powder: effects of cheese age, added dairy ingredients and spray drying temperature on properties of cheese powders, *J. Food Eng.* 237 (2018) 215–225, <https://doi.org/10.1016/j.jfoodeng.2018.05.015>.
- [11] M.-L. Vignolles, R. Jeantet, C. Lopez, P. Schuck, Free fat, surface fat and dairy powders: interactions between process and product. A review, *Lait* 87 (2007) 187–236, <https://doi.org/10.1051/lait:2007010>.
- [12] M.L. Vignolles, C. Lopez, M.N. Madec, J.J. Ehrhardt, S. Méjean, P. Schuck, R. Jeantet, Fat properties during homogenization, spray-drying, and storage affect the physical properties of dairy powders, *J. Dairy Sci.* 92 (2009) 58–70, <https://doi.org/10.3168/jds.2008-1387>.
- [13] K.P. Drapala, M.A.E. Auty, D.M. Mulvihill, J.A. O'Mahony, Influence of lecithin on the processing stability of model whey protein hydrolysate-based infant formula emulsions, *Int. J. Dairy Technol.* 68 (2015) 322–333, <https://doi.org/10.1111/1471-0307.12256>.
- [14] K.P. Drapala, M.A.E. Auty, D.M. Mulvihill, J.A. O'Mahony, Performance of whey protein hydrolysate-maltodextrin conjugates as emulsifiers in model infant formula emulsions, *Int. Dairy J.* 62 (2016) 76–83, <https://doi.org/10.1016/j.idairyj.2016.03.006>.
- [15] K.P. Drapala, M.A.E. Auty, D.M. Mulvihill, J.A. O'Mahony, Influence of emulsifier type on the spray-drying properties of model infant formula emulsions, *Food Hydrocoll.* 69 (2017) 56–66, <https://doi.org/10.1016/j.foodhyd.2016.12.024>.

- [16] K. Szulc, J. Nazarko, E. Ostrowska-Ligeza, A. Lenart, Effect of fat replacement on flow and thermal properties of dairy powders, *LWT Food Sci. Technol.* 68 (2016) 653–658, <https://doi.org/10.1016/j.lwt.2015.12.060>.
- [17] M. Grafton, C.E. Davies, I.J. Yule, J.R. Jones, Technical note: a comparison of shear tests using Carr-Walker and Schulze annular shear cells on commercial agricultural crushed limestone of New Zealand, *Trans. ASABE* 55 (2012) 1676–1680, <https://doi.org/10.13031/2013.42376>.
- [18] S. Brückner, Estimation of the background in powder diffraction patterns through a robust smoothing procedure, *J. Appl. Crystallogr.* 33 (2000) 977–979, <https://doi.org/10.1107/S002188980003617>.
- [19] A. Goldstein, G. Annor, V. Vamadevan, I. Tetlow, J.J.K. Kirkensgaard, K. Mortensen, A. Blennow, K.H. Hebelstrup, E. Bertoft, Influence of diurnal photosynthetic activity on the morphology, structure, and thermal properties of normal and waxy barley starch, *Int. J. Biol. Macromol.* 98 (2017) 188–200, <https://doi.org/10.1016/j.ijbiomac.2017.01.118>.
- [20] C. Gaiani, J. Scher, P. Schuck, S. Desobry, S. Banon, Use of a turbidity sensor to determine dairy powder rehydration properties, *Powder Technol.* 190 (2009) 2–5, <https://doi.org/10.1016/j.powtec.2008.04.042>.
- [21] D. Felix da Silva, L. Ahrné, F.H. Larsen, A.B. Hougaard, R. Ipsen, Physical and functional properties of cheese powders affected by sweet whey powder addition before or after spray drying, *Powder Technol.* 323 (2018) 139–148, <https://doi.org/10.1016/j.powtec.2017.10.014>.
- [22] A.B. Hougaard, A.G. Sijbrandij, C. Varming, Y. Ardö, R. Ipsen, Emulsifying salt increase stability of cheese emulsions during holding, *LWT Food Sci. Technol.* 62 (2015) 362–365, <https://doi.org/10.1016/j.lwt.2015.01.006>.
- [23] C. Varming, A.B. Hougaard, Y. Ardö, R. Ipsen, Stability of cheese emulsions for spray drying, *Int. Dairy J.* 39 (2014) 60–63, <https://doi.org/10.1016/j.idairyj.2014.05.005>.
- [24] M. Uргу, A. Türk, S. Ünlütürk, F. Kaymak-Ertekin, N. Koca, Milk fat substitution by Microparticulated protein in reduced-fat cheese emulsion: the effects on stability, microstructure, rheological and sensory properties, *Food Sci. Anim. Resour.* 39 (2019) 23–34, <https://doi.org/10.5851/ksfa.2018.e60>.
- [25] C. Gaiani, M. Morand, C. Sanchez, E.A. Tehrani, M. Jacquot, P. Schuck, R. Jeantet, J. Scher, How surface composition of high milk proteins powders is influenced by spray-drying temperature, *Colloids Surf. B: Biointerfaces* 75 (2010) 377–384, <https://doi.org/10.1016/j.colsurfb.2009.09.016>.
- [26] L.S. Rupp, M.S. Molitor, J.A. Lucey, Effect of processing methods and protein content of the concentrate on the properties of milk protein concentrate with 80% protein, *J. Dairy Sci.* (2018) 1–12, <https://doi.org/10.3168/jds.2018-14383>.
- [27] S.V. Crowley, I. Gazi, A.L. Kelly, T. Huppertz, J.A. O'Mahony, Influence of protein concentration on the physical characteristics and flow properties of milk protein concentrate powders, *J. Food Eng.* 135 (2014) 31–38, <https://doi.org/10.1016/j.jfoodeng.2014.03.005>.
- [28] D. Schulze, *Flow properties of powders and bulk solids*, Powders Bulk Solids, Springer, Berlin, Heidelberg 2008, pp. 321–333.
- [29] A.W. Jenike, *Storage and flow of solids*, *Bull. Univ. Utah.* 53 (1964).
- [30] G.V. Barbosa-Canovas, E. Ortega-Rivas, P. Juliano, H. Yan, *Food Powders* (2005) <https://doi.org/10.1007/0-387-27613-0>.
- [31] J.J. Fitzpatrick, K. Barry, P.S.M. Cerqueira, T. Iqbal, J. O'Neill, Y.H. Roos, Effect of composition and storage conditions on the flowability of dairy powders, *Int. Dairy J.* 17 (2007) 383–392, <https://doi.org/10.1016/j.idairyj.2006.04.010>.
- [32] J.J. Fitzpatrick, T. Iqbal, C. Delaney, T. Twomey, M.K. Keogh, Effect of powder properties and storage conditions on the flowability of milk powders with different fat contents, *J. Food Eng.* 64 (2004) 435–444, <https://doi.org/10.1016/j.jfoodeng.2003.11.011>.
- [33] B.E. Tiensa, S. Barbut, A.G. Marangoni, Influence of fat structure on the mechanical properties of commercial pate products, *Food Res. Int.* 100 (2017) 558–565, <https://doi.org/10.1016/j.foodres.2017.07.051>.
- [34] P.R. Ramel, A.G. Marangoni, Characterization of the polymorphism of milk fat within processed cheese products, *Food Struct.* 12 (2017) 15–25, <https://doi.org/10.1016/j.foostr.2017.03.001>.
- [35] H. Gliguel, C. Lopez, C. Michon, P. Lesieur, M. Ollivon, The viscoelastic properties of processed cheeses depend on their thermal history and fat polymorphism, *J. Agric. Food Chem.* 59 (2011) 3125–3134, <https://doi.org/10.1021/jf103641f>.
- [36] C. Lopez, V. Briard-Bion, E. Beaucher, M. Ollivon, Multiscale characterization of the organization of triglycerides and phospholipids in emmental cheese: from the microscopic to the molecular level, *J. Agric. Food Chem.* 56 (2008) 2406–2414, <https://doi.org/10.1021/jf0720382>.
- [37] C. Himawan, V.M. Starov, A.G.F. Stapley, Thermodynamic and kinetic aspects of fat crystallization, *Adv. Colloid Interf. Sci.* 122 (2006) 3–33, <https://doi.org/10.1016/j.cis.2006.06.016>.
- [38] G. Rizzo, J.E. Norton, I.T. Norton, Emulsifier effects on fat crystallisation, *Food Struct.* 4 (2015) 27–33, <https://doi.org/10.1016/j.foostr.2014.11.002>.
- [39] M. Cerdeira, V. Pastore, L.V. Vera, S. Martini, R.J. Candal, M.L. Herrera, Nucleation behavior of blended high-melting fractions of milk fat as affected by emulsifiers, *Eur. J. Lipid Sci. Technol.* 107 (2005) 877–885, <https://doi.org/10.1002/ejlt.200500257>.
- [40] D. Felix da Silva, L. Ahrné, R. Ipsen, A.B. Hougaard, Casein-based powders: characteristics and rehydration properties, *Compr. Rev. Food Sci. Food Saf.* 00 (2017) 1–15, <https://doi.org/10.1111/1541-4337.12319>.
- [41] S.V. Crowley, A.L. Kelly, P. Schuck, R. Jeantet, J.A.O. Mahony, *Adv. Dairy Chem.* (2016) <https://doi.org/10.1007/978-1-4939-2800-2>.
- [42] D. Felix, *Comprehensive Reviews in Food Science and Food Safety* Published by Wiley on Behalf of Institute of Food Technologists (the " Owner "), 2017.
- [43] J. Ji, J. Fitzpatrick, K. Cronin, M.A. Fenelon, S. Miao, The effects of fluidised bed and high shear mixer granulation processes on water adsorption and flow properties of milk protein isolate powder, *J. Food Eng.* 192 (2017) 19–27, <https://doi.org/10.1016/j.jfoodeng.2016.07.018>.
- [44] S.V. Crowley, B. Desautel, I. Gazi, A.L. Kelly, T. Huppertz, J.A. O'Mahony, Rehydration characteristics of milk protein concentrate powders, *J. Food Eng.* 149 (2015) 105–113, <https://doi.org/10.1016/j.jfoodeng.2014.09.033>.
- [45] M. Holse, F.H. Larsen, Å. Hansen, S.B. Engelsen, Characterization of marama bean (*Tylosema esculentum*) by comparative spectroscopy: NMR, FT-Raman, FT-IR and NIR, *Food Res. Int.* 44 (2011) 373–384, <https://doi.org/10.1016/j.foodres.2010.10.003>.